Published in "Journal of Colloid and Interface Science 339(2): 317-324, 2009"
which should be cited to refer to this work.

Environment-sensitive stabilisation of silver nanoparticles in aqueous solutions

Ilja K. Voets [a,*], Arie de Keizer [a], Peter M. Frederik [b], Reint Jellema [b], Martien A. Cohen Stuart [a]

[a] *Laboratory of Physical Chemistry and Colloid Science, Wageningen University, Dreijenplein 6, 6703 HB Wageningen, The Netherlands*
[b] *EM Unit, Pathologie, Universiteit Maastricht, Universiteitssingel 50, 6229 ER Maastricht, The Netherlands*

We describe the preparation and characterisation of inorganic–organic hybrid block copolymer silver nanoparticles via the preparation of spherical multi-responsive polymeric micelles of poly(*N*-methyl-2-vinyl pyridinium iodide)-*block*-poly(ethylene oxide), $P2MVP_{38}$-*b*-PEO_{211} and poly(acrylic acid)-*block*-poly(isopropyl acrylamide), PAA_{55}-*b*-$PNIPAAm_{88}$ in the presence of $AgNO_3$. Hence, the P2MVP and PAA segments were employed to fix Ag^+ ions within the micellar core (25 °C) or shell (60 °C), while the PEO segments ensured spontaneous reduction of Ag^+ ions into metallic Ag, as well as colloidal stabilisation. Spherical and elongated composite core–shell(–corona) nanoparticles (CNPs) were formed containing several small, spherical silver nanoparticles within the micellar core or shell. As the co-assembly of the oppositely charged copolymers into micelles is electrostatically driven, the CNPs can be destabilised by, for example, addition of simple salts, *i.e.*, the CNPs are stimuli responsive. CNP size and morphology control can be achieved via the preparation protocol. For example, heating to 60 °C, *i.e.*, above the PNIPAAm LCST, results in core–shell–corona CNPs with the Ag-NPs situated in the aggregate shell.

1. Introduction

The preparation of stable, monodisperse metallic nanoparticles has been topic of active research for many years. Nowadays, many researchers also employ polymer-assisted fabrication routes to prevent the particles from undergoing self-aggregation and chemical reactions; that is, to overcome stability problems related to the high surface energy of inorganic nanoparticles [1,2]. Metal precursors (or preformed nanoparticles) may be loaded or 'trapped' into already formed polymeric micelles, but alternatively, they may also be used to induce micellisation of the otherwise soluble block copolymers [2–6]. Via nucleation and growth processes within the composite nanoparticles (CNPs), the initially formed primary metal atoms may further aggregate into clusters, resulting in either one single colloid per micellar core or into several small colloids within a micellar core [7]. Recently, also bimetallic colloids have been formed in solution [8]. In general, the formation of the metal nanoparticles from the metal precursor typically involves the addition of a reducing agent (*e.g.*, $LiAlH_4$, $NaBH_4$, $H_2N–NH_2$, $LiBEt_3H$, or H_2) and semiconductor nanoparticles can be obtained by addition of H_2S to the metal precursors to form metal sulfides [1–3,6,9,10]. Various applications have been suggested for the resulting hybrid organic–inorganic particles, including their potential as quantum dots (*i.e.*, fluorescent nanoparticles) [1,8,9], catalysts [1,6,11], particle growth modifiers [5,12], and MRI contrast agents [13–15].

In aqueous solutions, electrostatically driven co-assembly of charged copolymers and oppositely charged metal precursors gives rise to the formation of so-called complex coacervate core micelles (C3Ms) [16], also known as polyion complex (PIC) micelles [17], block ionomer complexes (BIC) [18], and interpolyelectrolyte complexes (IPEC) [19]. Examples include Au- and Pt-NP formation in aqueous mixtures of P2VP-*b*-PEO and a wide variety of Au and Pt-NP precursors [6,20], comicellisation of γ-Fe_2O_3 and PTEA-*b*-PAAm [13], and $La(OH)_3$-NP formation in aqueous solutions containing La^{3+} ions and PAA-*b*-PAAm copolymers [5,21,22]. Inspired by the spontaneous formation of silver nanowires in the presence of PMAA-*b*-PEO [4], *i.e.*, without addition of a reducing agent, and the numerous studies on NP formation in the presence of P2VP and P4VP-containing copolymers (exhibiting a rather high affinity for many metal precursors due to the formation of coordination bonds between the metal ions and the pyridinium segments [6,7,23]), we decided to study Ag-NP formation in C3Ms consisting of poly(*N*-methyl-2-vinyl pyridinium iodide)-*block*-poly(ethylene oxide), $P2MVP_{38}$-*b*-PEO_{211} and poly(acrylic acid)-*block*-poly(isopropyl acrylamide), PAA_{55}-*b*-$PNIPAAm_{88}$. As suggested by Zhang et al. [4], the presence of PEO should ensure the spontaneous reduction of Ag^+ to Ag through oxidation of the oxyethylene groups, while the polyelectrolyte segments should coordinate with the Ag^+ ions, so that the C3Ms may serve as a template for the spontaneous formation of silver nanoparticles.

* Corresponding author. Present address: Adolphe Merkle Institute, University of Fribourg, Route de l'ancienne Papeterie, CH-1723 Marly 1, Switzerland. Fax: +41 263009624.

E-mail addresses: ilja.voets@unifr.ch (I.K. Voets), arie.dekeizer@wur.nl (A. de Keizer), peter.frederik@elmi.unimaas.nl (P.M. Frederik), Reint.Jellema@KG.unimaas.nl (R. Jellema), martien.cohenstuart@wur.nl (M.A. Cohen Stuart).

In a previous publication [24], we have shown that micelles of P2MVP$_{38}$-*b*-PEO$_{211}$ and PAA$_{55}$-*b*-PNIPAAm$_{88}$ are responsive to a number of experimental parameters, such as pH, ionic strength, and temperature. The C3Ms reversibly associate and dissociate upon cycling the ionic strength of the solution through the so-called "critical ionic strength" (corresponding to the ionic strength above which micelles can no longer be detected), which is approximately 105 mM for this particular system [24]. Upon raising the temperature from 25 °C to 60 °C, the C3Ms undergo a structural transition from core–shell C3Ms at T = 25 °C with the polyelectrolyte blocks in the core to a core–shell–corona system at T = 60 °C with the polyelectrolyte blocks in the shell. In the present contribution, we will demonstrate that the responsive nature of complex coacervate core micelles renders them an attractive candidate for polymer-assisted fabrication and stabilisation of silver nanoparticles (Ag-NPs). We will show that the size and location of Ag-NPs within the micellar carrier can be controlled through preparation of the complexes at various temperatures as these are coupled to distinct morphologies of the micelles and hence, different loci of the polyelectrolyte segments to which the Ag-NPs are coordinated. Furthermore, we will show that a controlled release of Ag-NPs is easily achieved through the addition of a simple monovalent salt $NaNO_3$.

In the following, we will refer to the silver nanoparticles with the abbreviations (Ag-)NPs, to the micellar carriers as (complex coacervate core) micelles, C3Ms, or carriers, and to the combination of Ag-NPs and C3Ms as hybrid organic–inorganic nanoparticles and composite nanoparticles (CNPs).

2. Materials and methods

2.1. Materials

Poly(*N*-methyl-2-vinyl pyridinium iodide)-*block*-poly(ethylene oxide), P2MVP$_{38}$-*b*-PEO$_{211}$ (M_w = 13 kg mol^{-1}) has been synthesised by sequential anionic polymerisation [25,26] (polydispersity index, PDI ~ 1.01), followed by quaternisation with methyl iodide (degree of quaternisation ~89%). Poly(acrylic acid)-*block*-poly(isopropyl acrylamide), PAA$_{55}$-*b*-PNIPAAm$_{88}$ (M_w = 14 kg mol^{-1}) has been synthesised by RAFT (PDI ~ 1.10), according to a procedure described elsewhere [24,27]. All polymers and other chemicals were used as received, without further purification. Chemical structures are given in Scheme 1 [Subscripts correspond to the degree of polymerisation].

2.2. Sample preparation

Aqueous polymer stock solutions were prepared by dissolution of known amounts of polymer into Milli-Q water to which $NaNO_3$ was added to obtain [$NaNO_3$] = 1 mM, followed by a pH-adjustment to pH = 7.7 ± 0.1 using 0.1 and 1.0 M NaOH and HNO_3. The stock solutions were mixed in a 1:1 ratio of chargeable groups; *i.e.*, at a mixing fraction, f_+ of 0.5. For pH = 7.7, this mixing fraction corresponds to the so-called preferred micellar composition (PMC) [24]. The mixing fraction, f_+ is defined as the ratio between the number of positively chargeable monomers and the sum of the numbers of positively and negatively chargeable monomers, *i.e.*,

$$f_+ = \frac{[n_+]}{[n_+] + [n_-]}$$

The control samples A, B, and C were prepared by mixing the filtered P2MVP$_{38}$-*b*-PEO$_{211}$ and PAA$_{55}$-*b*-PNIPAAm$_{88}$ stock solutions (1× over a 0.45 μm Schleicher and Schuell filter). The samples D, E, F, and K were prepared by mixing the filtered P2MVP$_{38}$-*b*-PEO$_{211}$ and PAA$_{55}$-*b*-PNIPAAm$_{88}$ stock solutions, followed by addition of an excess of $AgNO_3$ (*e.g.*, [Ag^+] ≫ [P2(M)VP]), and centrifugation for at least 20 min at 13,000 rpm, to remove the precipitated AgI formed through complexation of Ag^+ with the P2MVP$^+$ counterions, *i.e.*, I^-. The supernatant was decanted into a vial and $AgNO_3$ was again added in excess (*e.g.*, [Ag^+] ≫ [P2(M)VP]). Now, no more precipitation is observed, indicating that in the previous step all I^- counterions have been replaced by NO_3^- counterions. The control samples A, B, and C without silver ions, and the samples D, E, F, and K with silver ions were placed in the fridge (A, D, K) or in a programmable thermostated bath. Silver containing P2MVP$_{38}$-*b*-PEO$_{211}$ stock solutions for samples H and J were prepared by addition of $AgNO_3$ to the filtered P2MVP$_{38}$-*b*-PEO$_{211}$ stock solution, followed by the same procedure as used in the preparation of samples D, E, and F to get rid of the insoluble salt AgI. The stock solutions of P2MVP$_{38}$-*b*-PEO$_{211}$ and PAA$_{55}$-*b*-PNIPAAm$_{88}$ for the control samples G and I without silver ions, and for the samples H and J with silver ions were placed in the fridge (G, H) or in the thermostated bath (I, J). Sample B was heated from 25 °C to 60 °C with a rate of 0.03 °C min^{-1}, while the samples C, E, F, and the stock solutions for the samples I and J were kept at 33 °C for 23 h, followed by heating from 33 °C to 60 °C in ~25 min. The P2MVP$_{38}$-*b*-PEO$_{211}$ and PAA$_{55}$-*b*-PNIPAAm$_{88}$ stock solutions for samples G, H, I, and J were mixed at T = 25 (G, H) and 60 °C (I, J) one full day after storage in the fridge or the thermostated bath. A concentrated $NaNO_3$ solution
was added to samples C and F ~36 h after their preparation. A summary of the preparation protocol of the various samples is given in Table 1.

2.3. Dynamic light scattering (DLS)

Dynamic light scattering measurements have been performed on (1) an ALV light scattering instrument equipped with an ALV-5000/60 × 0 digital correlator and a Lexel 85 400 mW argon ion laser operated at a wavelength of 514.5 nm, on (2) an ALV light scattering instrument equipped with an ALV-5000 digital correlator and a Spectra Physics 2000 1 W argon ion laser operated at a wavelength of 514.5 nm, and on (3) an ALV light scattering instrument equipped with an ALV-5000 digital correlator and a 100 mW DPSS laser operated at a wavelength of 532 nm. In all three setups, a refractive index matching bath of filtered *cis*-decalin

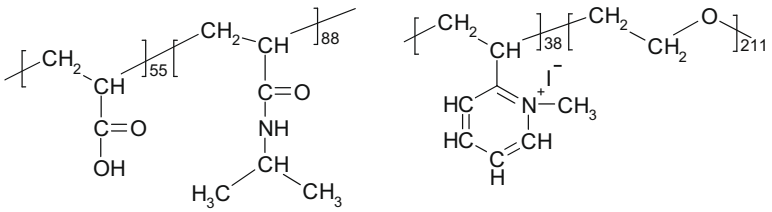

Scheme 1. Chemical structure of the polymers used in this study. (Left) Poly(acrylic acid)-*block*-poly(isopropyl acrylamide), PAA$_{55}$-*b*-PNIPAAm$_{88}$; (right) poly(*N*-methyl-2-vinyl pyridinium iodide)-*block*-poly(ethylene oxide), P2MVP$_{38}$-*b*-PEO$_{211}$. Note that 38 denotes the sum of the number of quaternised and non-quaternised monomers (~11%). The numbers beside the brackets denote the degree of polymerisation.

Table 1
Overview of the various samples in this study (see also text for further details). $AgNO_3$ was added after C3M formation in samples D, E, F, and K, while $AgNO_3$ was added to the $P2MVP_{38}$-*b*-PEO_{211} stock solution prior to C3M formation in samples H and J. Samples A, B, C, G, and I are control samples for D, K (A), E (B), F (C), H (G), and J (I) to which no $AgNO_3$ is added. [a] Radii are given in nanometres, the ionic strength is given in mM.

Sample	$AgNO_3$	t_{AgNO_3}	$[NaNO_3]$	$T_{formation}$	$T_{storage}$	$R_{h,90°}$[d]	$R_{h,90°}$[e]
A	Control (D, K)	–	1	25	25	18.2 ± 0.3	19.3 ± 0.4
B	Control (E)	–	1	25[c]	60	47.2 ± 0.7	56.7 ± 1.0
C	Control (F)	–	$>I_{cr}$	25[c]	60	58.6 ± 1.7	–
D[f]	$AgNO_3$	to C3Ms	1	25	25	64.2 ± 1.0	104.8 ± 2.9
K[f]	$AgNO_3$	to C3Ms	1	25	25	23.8 ± 0.3	93.1 ± 2.6
E	$AgNO_3$	to C3Ms	1	25[c]	60	98.0 ± 3.1	118.0 ± 9.0
F	$AgNO_3$	to C3Ms	$>I_{cr}$	25[c]	60	123.6 ± 6.3	–
G	control (H)	–	1	25	25	–	19.6 ± 0.7
H	$AgNO_3$	to $P2MVP_{38}$-*b*-PEO_{211}	1	25	25	–	60.6 ± 0.7
I	control (J)	–	1	60[b,c]	60	–	63.6 ± 1.6
J	$AgNO_3$	to $P2MVP_{38}$-*b*-PEO_{211}	1	60[b,c]	60	–	89.6 ± 5.6

[a] The column t_{AgNO_3} reads 'to C3Ms' when $AgNO_3$ was added after C3M formation, while 'to $P2MVP_{38}$-*b*-PEO_{211}' denotes $AgNO_3$ addition prior to C3M formation. The column $AgNO_3$ denotes 'control' if no $AgNO_3$ was added to the sample and '$AgNO_3$' if $AgNO_3$ was added to the sample. $T_{formation}$/°C refers to the temperature at which the C3Ms were prepared, i.e., the temperature at which the P2MVP-*b*-PEO and PAA-*b*-PNIPAAm stock solutions were mixed. $T_{storage}$/°C corresponds to the temperature at which the C3Ms were stored after preparation, i.e., after mixing the P2MVP-*b*-PEO and PAA-*b*-PNIPAAm stock solutions.

[b] A premixed Ag^+/P2MVP-*b*-PEO solution was added to a PAA-*b*-PNIPAAm stock solution (stored at 33 °C for 23 h, followed by heating from 33 °C to 60 °C in ~25 min), so that PAA-*b*-PNIPAAm had already formed micelles with a PNIPAAm core and a PAA corona, as $T_f > LCST_{PNIPAAm}$.

[c] Sample B was heated from 25 °C to 60 °C with a rate of 0.03 °C min^{-1}, while the samples C, E, F, and the stock solutions for the samples I and J were kept at 33 °C for 23 h, followed by heating from 33 °C to 60 °C in ~25 min.

[d] DLS measurements were performed ~3 days after C3M formation in samples A–F, and K, and prior to addition of $NaNO_3$ to raise $[NaNO_3] > I_{cr}$ in samples C and F.

[e] DLS measurements were performed ~7 days after C3M formation in samples A–F, and K, and ~4 days after C3M formation in samples G–J and addition of $NaNO_3$ to raise $[NaNO_3] > I_{cr}$ in samples C and F.

[f] Samples D and K are identical, but $AgNO_3$ was added on different times after C3M formation to be able to follow the kinetics of Ag nanoparticle formation more carefully. See text and caption to Fig. 4 for further details.

surrounded the cylindrical scattering cell, and the temperature was controlled using (1) a Haake F8-C35 thermostat, (2) a Haake F3-K thermostat, and (3) a Haake Phoenix II-C25P thermostat.

The second-order correlation function, $G_2(t)$, was recorded 5 times per angle, θ, at $\theta = 90°$ or at 19 angles ($35° < \theta < 135°$, increments of 5°) to evaluate the angular dependence of the diffusion coefficient, D. DLS experiments have been analysed using the method of cumulants. The diffusion coefficient extrapolated to zero angle, $D°$, has been obtained from the slope in a plot of the average frequency, Γ versus q^2 and has been calculated into a hydrodynamic radius, R_h^0 via the Stokes–Einstein equation.

2.4. Cryogenic transmission electron microscopy (cryo-TEM)

Cryo-TEM observations were carried out at 100 K on a Philips CM12 Microscope operating on at 120 kV. Samples were prepared on Quantifoil® grids (R2/2, 200 mesh grids with a pattern of 2 μm holes in a support film) using the Vitrobot®. Images were taken under low dose conditions. For details see [28]. Samples A, D, G, H, K, and $AgNO_3$ containing $P2MVP_{38}$-*b*-PEO_{211} solution for sample H were blotted at $T = 25$ °C. Samples B, E, I, J, and $AgNO_3$ containing $P2MVP_{38}$-*b*-PEO_{211} solution for sample J were blotted at $T = 60$ °C. In between storage and blotting, the temperature was carefully kept at $60 \leqslant T \leqslant 65$ °C. Blotting was performed at least 96 h after the last sample preparation step, *i.e.*, either mixing of the (Ag-containing) $P2MVP_{38}$-*b*-PEO_{211} and PAA_{55}-*b*-$PNIPAAm_{88}$ stock solutions (samples A, B, G, H, I, and J) or addition of $AgNO_3$ to the preformed C3M solutions (samples D, E, and K).

3. Results and discussion

3.1. Micelle formation in the absence of $AgNO_3$

As reported previously, spherical micelles ($R_h^0 = 13.6$ nm) are formed spontaneously in aqueous mixtures of $P2MVP_{38}$-*b*-PEO_{211} and PAA_{55}-*b*-$PNIPAAm_{88}$ at $T = 25$ °C [24]. They appear to be in coexistence with a (small) number of large (loose) aggregates, as a 'fast' and a 'slow' mode is observed in dynamic light scattering (DLS) experiments. From static light scattering (SLS) experiments, the C3Ms were found to consist of about 16 cationic and 11 anionic copolymers. Upon addition of $NaNO_3$, the C3Ms were found to swell until above ~105 mM $NaNO_3$ micelles could no longer be detected. Temperature-induced aggregation was observed upon raising the temperature from 25 °C to temperatures above the LCST of PNIPAAm (~33 °C). Aggregate size and mass were found to be dependent on temperature, and for fast scan rates (>0.03 °C min^{-1}), on scan rate and history. The aggregate structure at 60 °C was found to be of the 'core–shell–corona' type; *i.e.*, the aggregates consist of a PNIPAAm core, surrounded by a coacervate shell, stabilised by a PEO corona. Cryo-TEM images on the control samples A ($T = 25$ °C) and B ($T = 60$ °C), *i.e.*, in the absence of $AgNO_3$, are presented in Fig. 1. The greyish dots in Fig. 1a, corresponding to the micellar cores of the core–shell C3Ms in sample A ($T_f = T_s \leqslant 25$ °C), are much smaller ($R \sim 4$ nm) than those observed in Fig. 1b ($R \sim 16$ nm), corresponding to the aggregate core (and possibly shell) of the core–shell–corona micelles in sample B, which was heated from 25 °C to 60 °C with a rate of 0.03 °C min^{-1} shortly after mixing the polymer stock solutions.

3.2. Nanoparticle formation within preformed C3Ms

Upon addition of $AgNO_3$ to the preformed C3Ms depicted in Fig. 1a so that $[Ag^+] \gg [P2(M)VP]$, precipitation occurs, as an insoluble AgI salt is formed due to complexation of Ag^+ with I^- ions (see materials and methods section). After removal of this precipitate, further addition of $AgNO_3$ does not result in precipitation. In analogy to the coordination of Ag^+ with PMAA segments and Au and Pt-NP precursors with P2VP segments in aqueous mixtures of PMAA-*b*-PEO/Ag^+ [4] and P2VP-*b*-PEO/Au and Pt-NP precursors [6,20], silver ions are now selectively incorporated into the C3M cores as they contain pyridinium and acid groups. This results in the spontaneous (that is, without the addition of a reducing agent) formation of silver nanoparticles within the C3Ms, as manifested by a gradual yellowish/reddish coloration of the Ag-containing solutions in samples D and K (Fig. 2). In the cryo-TEM images, we observe tiny dark dots corresponding to silver nanoparticles

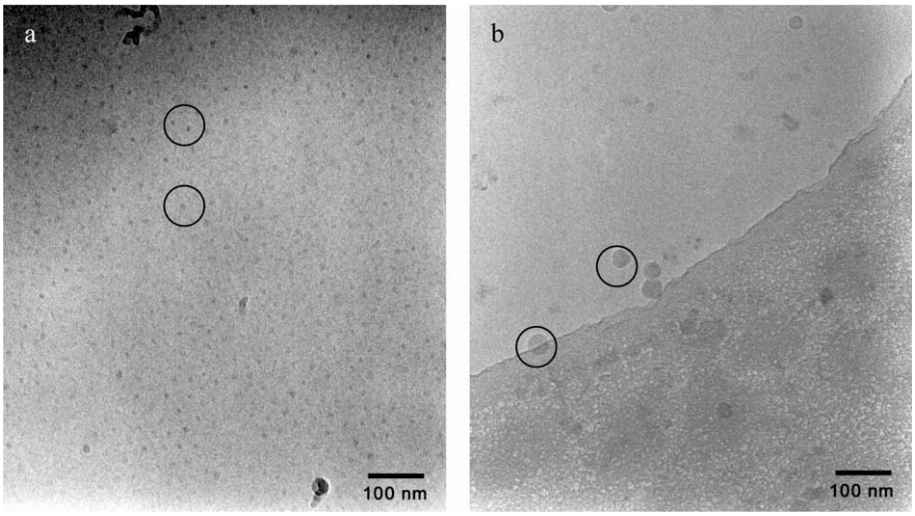

Fig. 1. Cryo-TEM images of a 1:1 mixture of $P2MVP_{38}$-*b*-PEO_{211} and PAA_{55}-*b*-$PNIPAAm_{88}$ at: (a) $T = 25$ °C (sample A) and (b) $T = 60$ °C (sample B). The black circles indicate core–shell C3Ms in sample A and core–shell–corona micelles in sample B.

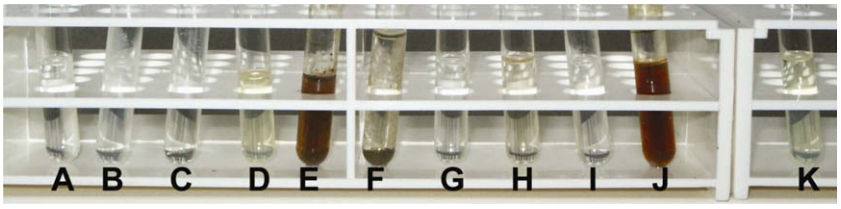

Fig. 2. Pictures of samples A–K, taken over 10 days after micellisation. The sample codes correspond to those given in Table 1. Ag-NP formation is manifested by a yellowish/reddish coloration of the Ag-containing samples, being samples D, E, F, H, J, and K. Precipitation of the Ag-NPs is observed after addition of $NaNO_3$ to raise $[NaNO_3] > I_{cr}$ (sample F), while no precipitation is visible for $[NaNO_3] = 1$ mM (sample E). (For interpretation of color mentioned in this figure the reader is referred to the web version of the article.)

($R < 4$ nm) and larger greyish spots corresponding to the C3M cores (Fig. 3). Clearly, there is quite some variation in particle size, aggregation state, and shape. In both images, (near) spherical, as well as elongated (open arrows), worm-like structures can be observed. Besides, there is a non-negligible amount of approximately spherical objects of considerably higher (circles) and lower (closed arrows) contrast than average. These results are in agreement with the DLS measurements, where $R_{h,90°}$ was found to be larger for samples D and K than for sample A (Table 1). Moreover, deviations from linearity are observed in R_h^0 versus q^2 in the low-q region (cumulant analysis of DLS results), which are caused by the presence of a (small) number of large (loose) aggregates as observed

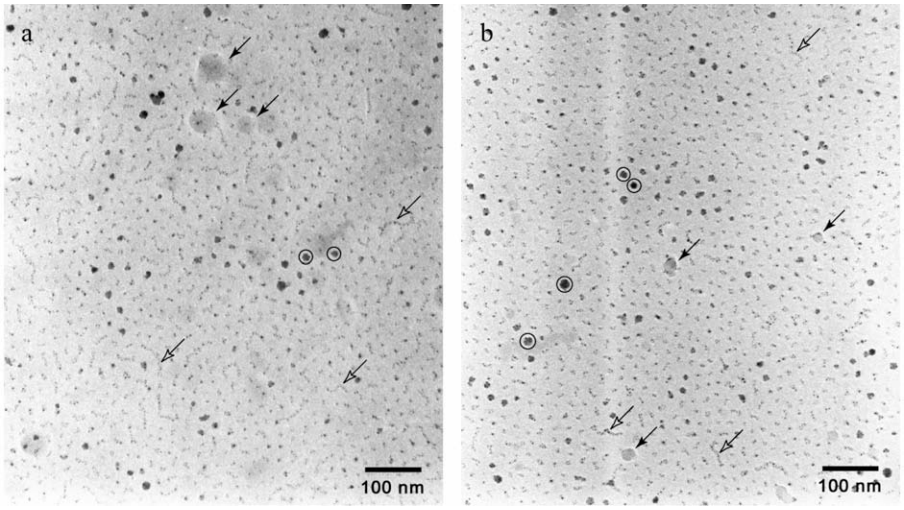

Fig. 3. Cryo-TEM images of a 1:1 mixture of $P2MVP_{38}$-*b*-PEO_{211} and PAA_{55}-*b*-$PNIPAAm_{88}$ in the presence of $AgNO_3$ at $T = 25$ °C. The sample was blotted: (a) ~8 days (sample D) and (b) ~7 days (sample K) after addition of $AgNO_3$. Circles and closed arrows indicate approximately spherical objects of considerably higher (circles) and lower (arrows) contrast than average. Several elongated, worm-like structures are indicated with open arrows. Note that the two samples are very similar, although they correspond to a 24 h difference in Ag^+ addition. Note that – on the contrary – these images are very different from those obtained for samples prepared at 60 °C as shown in Fig. 5.

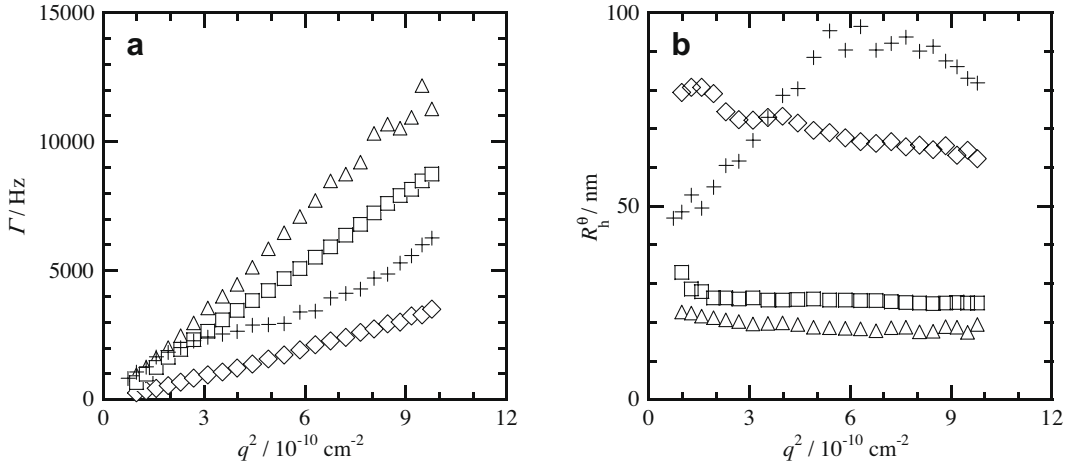

Fig. 4. Cumulant results. (a) Γ as a function of q^2 and (b) R_h^θ as a function of q^2 for (Δ) sample A, 3 days after C3M formation in absence of Ag^+, (◇) sample D, 3 days after C3M formation, ~52 h after addition of Ag^+, (□) sample K, 3 days after C3M formation, ~29 h after addition of Ag^+, and (+) sample J, 6 days after addition of Ag^+ to the $P2MVP_{38}$-*b*-PEO_{211} stock solution, and ~64 h after C3M formation.

previously [24], and/or non-spherical particles (Fig. 4). Samples A and K show the smallest deviation from linearity, consistent with the fact that the smallest amount of aggregates and/or non-spherical particles was observed in the cryo-TEM images of these samples, and furthermore, they contain the smallest particles, and are thus closest to the Rayleigh limit ($R < \lambda/20$).

The NP induced increase in $R_{h,90°}$ is a rather slow process, occurring on a timescale of several days. For example, about 3 days after C3M formation and 29 h after addition of Ag^+, $R_{h,90°} \sim 23.8 \pm 0.3$ nm (sample K), while after 52 h, $R_{h,90°} \sim 64.2 \pm 1.0$ nm (sample D). About 7 days after C3M formation, and 132 h after addition of Ag^+, $R_{h,90°} \sim 93.1 \pm 2.6$ nm, while after 155 h, $R_{h,90°} \sim 104.8 \pm 2.9$ nm. The particles continue to grow for several days, but the absolute difference in particle size becomes smaller with increasing time after Ag^+ addition, indicating the existence of a maximum particle size. While the Ag-NPs appear to be randomly distributed within the micellar cores of about 8 nm in diameter, they are mostly found at the periphery of the larger and darker spherical objects (circles). The slow kinetics and random Ag-NP distribution is in agreement with the results of Zhang et al., who observed Ag-NP formation within an aging time of 5 h in the PMAA-*b*-PEO/Ag^+ system. Contrary to their system, where the formation of smooth silver nanowires was observed after >54 h of aging, we do not observe aggregation into clusters of continuous Ag-NPs. Still, some elongated, worm-like objects containing several separated Ag-NPs are clearly observed. One might hypothesise that NP formation at a different f_+ may lead to the incorporation of a larger number of silver ions, and could thus potentially lead to the formation of continuous metal nanowires.

The encircled aggregates in Fig. 3 resemble the objects found in sample E (Fig. 5), where the first stages of NP formation take place at 33 °C, as the sample was kept at 33 °C for 23 h, followed by heating from 33 °C to 60 °C in ~25 min. Here, most objects appear spherical with $R \sim 7$–10 nm, containing small NPs on the periphery, confirming the core–shell–corona structure of $P2MVP_{38}$-*b*-PEO_{211} and PAA_{55}-*b*-$PNIPAAm_{88}$ aggregates at elevated temperatures. As Ag^+ coordinates with the PAA and/or P2(M)VP monomers in the coacervate layer, the NPs should be formed at the periphery of the core, *i.e.*, in the shell of the core–shell–corona particles, where they are indeed observed. The cryo-TEM images suggest that the cores of the CNPs of sample E are smaller than those of sample B, *i.e.*, 14–20 nm instead of ~32 nm, in agreement with our previous findings on aqueous mixtures of $P2MVP_{38}$-*b*-PEO_{211} and PAA_{55}-*b*-$PNIPAAm_{88}$ in the absence of Ag^+, where quick

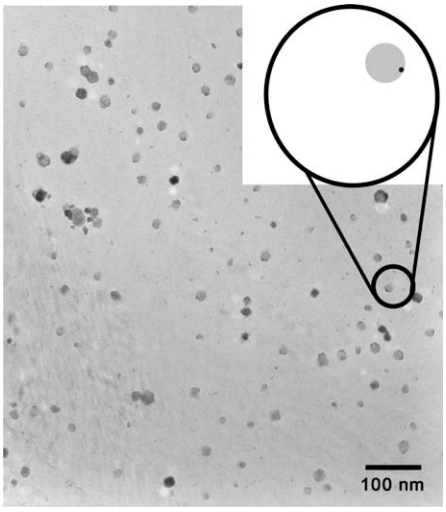

Fig. 5. Cryo-TEM image of sample E. $AgNO_3$ was added to a 1:1 mixture of $P2MVP_{38}$-*b*-PEO_{211} and PAA_{55}-*b*-$PNIPAAm_{88}$, followed by storage at 33 °C for 23 h and consecutive heating from 33 °C to 60 °C in ~25 min. The sample was blotted at $T = 60$ °C for ~7 days after addition of $AgNO_3$. The inset is a schematic representation of a core–shell–corona particle containing one silver nanoparticle in the shell.

heating to 60 °C resulted in smaller particle sizes [24]. However, Table 1 shows that, 3 days after C3M formation, the $R_{h,90°}$ of CNPs (sample E, F) are larger than those of the aggregates without Ag-NPs (sample B, C). A tentative explanation might be that there is an increased tendency for secondary aggregation in the Ag-containing samples due to the oxidation of the oxyethylene groups. As observed for the CNPs at $T = 25$ °C, $R_{h,90°}$ increases with increasing time after Ag^+ addition.

3.3. Nanoparticle formation after premixing Ag^+ and P2MVP-b-PEO

Fig. 6 shows cryo-TEM images of samples G and H ($T = 25$ °C), where G is the control sample, *i.e.*, in the absence of Ag^+, and H is the sample where C3M formation occurred after premixing of Ag^+ and $P2MVP_{38}$-*b*-PEO_{211}. Both images depict objects of $R \sim 4$ nm (approximately the same size as in Fig. 1a), while in Fig. 1b we can again clearly observe the NP formation. However, contrary to samples D and K (Fig. 3), nearly all objects are spherical, and hardly any elongated, worm-like structures are observed. As ob-

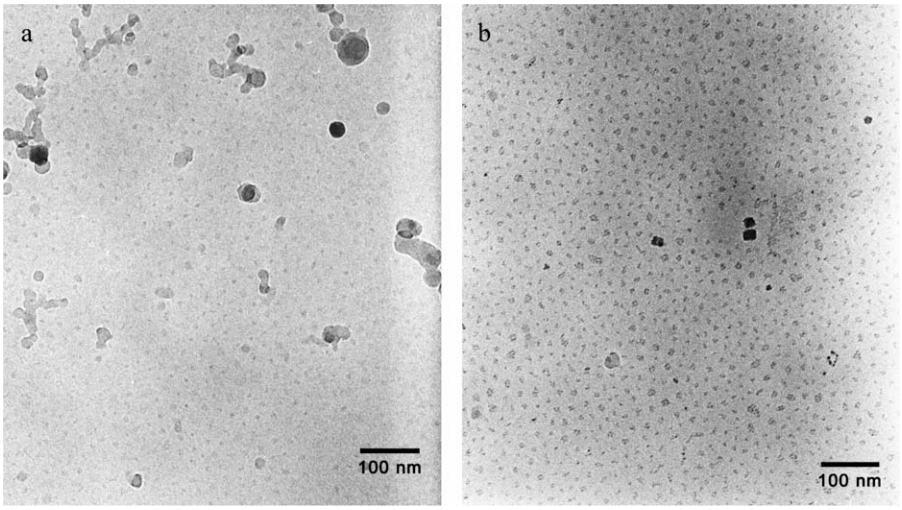

Fig. 6. Cryo-TEM images of a 1:1 mixture of $P2MVP_{38}$-*b*-PEO_{211} and PAA_{55}-*b*-$PNIPAAm_{88}$: (a) in the absence (sample G) and (b) in the presence (sample H) of $AgNO_3$ at $T = 25$ °C. Sample H was blotted ~8 days after addition of $AgNO_3$ to the $P2MVP_{38}$-*b*-PEO_{211} stock solution, and ~6 days after mixing the stock solutions of cationic and anionic polymers (i.e., ~52 h passed between addition of $AgNO_3$ to the $P2MVP_{38}$-*b*-PEO_{211} stock solution and mixing of the stock solutions).

served for Ag-NP formation after C3M formation, premixing of Ag^+ with $P2MVP_{38}$-*b*-PEO_{211} before C3M formation results in CNPs with larger $R_{h,90°}$ than the corresponding C3Ms without Ag-NPs (*i.e.*, compare $R_{h,90°}$ of samples H and G, and those of samples D, K, and A).

When C3M formation occurred at $T = 60$ °C after premixing of Ag^+ and $P2MVP_{38}$-*b*-PEO_{211} (Sample J, Fig. 7b), *i.e.*, after formation of PAA_{55}-*b*-$PNIPAAm_{88}$ micelles with a hydrophobic PNIPAAm core and a negatively charged PAA corona, large aggregates of $R \sim 16$ nm are observed, as in the control sample I (Fig. 7a) in absence of Ag^+, and in addition tiny dark spots corresponding to Ag-NPs, larger and darker than in samples D, K, H (where micellisation occurred at $T = 25$ °C), and sample E (where micellisation occurred at $T = 60$ °C). Contrary to those samples, there is a considerable amount of Ag-NPs that appear not to be associated with the aggregate cores, *i.e.*, they are not found within or on the periphery of the objects, but are seemingly 'free'. This is in agreement with the observation of (partial) macroscopic precipitation in sample J, as the free Ag-NPs, *i.e.*, without stabilisation by polymer micelles, are colloidally instable.

3.4. Environment-sensitive stabilisation

In the previous sections, we have shown that composite nanoparticles (CNPs) consisting of two oppositely charged block copolymers $P2MVP_{38}$-*b*-PEO_{211} and PAA_{55}-*b*-$PNIPAAm_{88}$ and Ag-NPs are formed spontaneously, *i.e.*, without addition of a reducing agent, in aqueous solutions. We have demonstrated possibilities to tune the size of the Ag-NPs, the size and shape of the composite nanoparticles, and the location of the Ag-NPs within the CNPs. Key parameters are the temperature at which the CNPs are prepared and the order of mixing of the individual components. At room temperature, upon addition of Ag^+ after comicellisation of the block copolymers, the resulting core–shell CNPs contain

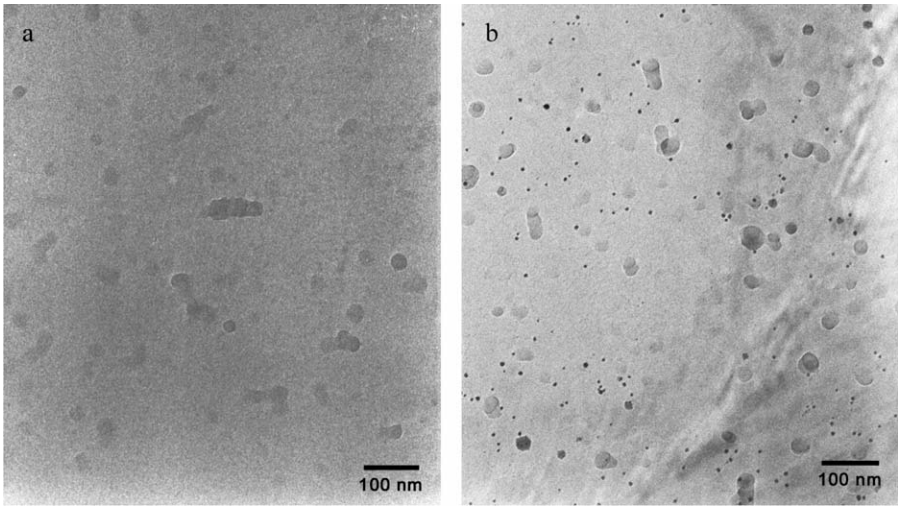

Fig. 7. Cryo-TEM images of a 1:1 mixture of $P2MVP_{38}$-*b*-PEO_{211} and PAA_{55}-*b*-$PNIPAAm_{88}$: (a) in the absence (sample I) and (b) in the presence (sample J) of $AgNO_3$ at $T = 60$ °C. Sample J was blotted ~8 days after addition of $AgNO_3$ to the $P2MVP_{38}$-*b*-PEO_{211} stock solution, and ~6 days after mixing the stock solutions of cationic and anionic polymers at $T = 60$ °C (i.e., ~52 h passed between addition of $AgNO_3$ to the $P2MVP_{38}$-*b*-PEO_{211} stock solution and mixing of the stock solutions). See also Fig. 4 for DLS experiments on this sample.

several small Ag-NPs in the micellar core of spherical and worm-like micelles (samples D and K). Upon premixing Ag^+ and P2MVP$_{38}$-*b*-PEO$_{211}$, followed by addition of this solution to the PAA$_{55}$-*b*-PNIPAAm$_{88}$ solution, the resulting CNPs are of comparable size, but now nearly all objects are spherical and hardly any elongated, worm-like structures are observed (sample H). When the C3Ms formed at room temperature are heated to $T = 60$ °C in the presence of Ag^+, the resulting core–shell–corona CNPs are larger and contain several Ag-NPs in the micellar shell (sample E). Upon premixing Ag^+ and P2MVP$_{38}$-*b*-PEO$_{211}$, and addition of this solution to a PAA$_{55}$-*b*-PNIPAAm$_{88}$ solution at $T = 60$ °C, *i.e.*, containing preformed PAA$_{55}$-*b*-PNIPAAm$_{88}$ micelles (sample J), similar core–shell–corona CNPs are formed containing larger Ag-NPs, in coexistence with a considerable amount of non-associated 'free' Ag-NPs, leading to (partial) macroscopic precipitation.

In the previous sections, we have characterised the thermo-sensitivity of the complexes of Ag-NP, PAA$_{55}$-*b*-PNIPAAm$_{88}$ and P2MVP$_{38}$-*b*-PEO$_{211}$ and utilised this feature to prepare CNPs of different size and shape containing several Ag-NPs within their core or shell. As the complexes are formed by virtue of electrostatics (Coulombic attraction and entropy gain through counterion release), they are also pH and salt-sensitive [16,24,29–31]. The former arises from the weak (annealed) nature of the PAA segments; that is, their charge is dependent on pH. As a consequence, we can destabilise the CNPs by addition of a sufficiently large amount of acid, such as HCl, or salt, such as $NaNO_3$. To demonstrate this environment-responsive character, we have prepared two identical samples E and F, containing a colloidally stable mixture of Ag^+, P2MVP$_{38}$-*b*-PEO$_{211}$, and PAA$_{55}$-*b*-PNIPAAm$_{88}$. To one of these samples, sample F, we have added a large amount of $NaNO_3$ such that the ionic strength exceeds the so-called critical ionic strength (but not the solubility limit of $AgNO_3$), above which electrostatic interactions become screened to the extent that the driving force for micellisation vanishes. Consequently, the CNPs disintegrate releasing the Ag-NPs into the solution. As these are no longer sterically stabilised by a surrounding layer of swollen polymer segments, the Ag-NPs precipitate. A macroscopic two-phase system is now formed with the heavy Ag-NPs in the bottom phase, as can be detected from the dark coloration in the bottom of the test tube in sample F (Fig. 2). On the contrary, in sample E, the CNPs are colloidally stable and homogeneously dispersed throughout the sample volume resulting in a coloration of the entire sample.

4. Conclusion

We have reported on the formation of silver containing composite nanoparticles (CNPs) consisting of silver nanoparticles (Ag-NPs), poly(*N*-methyl-2-vinyl pyridinium iodide)-*block*-poly(ethylene oxide), P2MVP$_{38}$-*b*-PEO$_{211}$ and poly(acrylic acid)-*block*-poly(isopropyl acrylamide), PAA$_{55}$-*b*-PNIPAAm$_{88}$. Both the Ag-NPs and the CNPs from spontaneously upon mixing of the double hydrophilic block copolymers in the presence of silver ions; that is, without the addition of a reducing agent such as $NaBH_4$. We have demonstrated possibilities to achieve control over the size of the Ag-NPs, the size and shape of the CNPs, and the location of the Ag-NPs within the CNPs. Spherical and elongated CNPs were observed. Ag-NPs were found to colocalise with the polyelectrolyte blocks within the CNPs. Temperature could be used to trigger a structural transition from a core–shell structure at $T = 25$ °C to a core–shell–corona structure at $T = 60$ °C , translocating the Ag-NPs from the micellar core in the former into the micellar shell in the latter. The most uniform and well-defined CNPs were obtained by premixing Ag^+ and P2MVP$_{38}$-*b*-PEO$_{211}$ at room temperature prior to addition of this solution to a solution of PAA$_{55}$-*b*-PNIPAAm$_{88}$ at $T = 25$ °C (sample H). Finally, we have shown that the colloidal stability of the CNPs is dependent on the ionic strength of the solution: Ag-NP release from the CNPs can easily be triggered by addition of a simple salt, such as $NaNO_3$.

In summary, this work shows that complex coacervate core micelles can be regarded as a promising candidate for polymer-assisted synthesis and stabilisation of silver nanoparticles. Future work might be directed towards the potential application of such CNPs as environment-sensitive silver quantum dots and as antimicrobial agents in antifouling surface coatings that can be prepared upon exposure of hydrophilic surfaces to a solution of Ag-NP containing CNPs [32].

Acknowledgments

We would like to thank Holger Schmalz and Christophe Detrembleur for the synthesis of the copolymers, and Remco Fokkink for his contributions to the light scattering measurements. This work is part of the research programme of the Stichting voor Fundamenteel Onderzoek der Materie (FOM), which is financially supported by the Nederlandse Organisatie voor Wetenschappelijk Onderzoek (NWO). This study has been carried out in the framework of the EU Polyamphi/Marie Curie Program (FP6-2002, Proposal 505027). IV was financed by the SONS Eurocores program (Project JA16-SONS-AMPHI).

References

[1] B.A. Rozenberg, R. Tenne, Progress in Polymer Science 33 (2008) 40.
[2] G. Riess, Progress in Polymer Science 28 (2003) 1107.
[3] M. Antonietti, S. Forster, J. Hartmann, S. Oestreich, Macromolecules 29 (1996) 3800.
[4] D.B. Zhang, L.M. Qi, J.M. Ma, H.M. Cheng, Chemistry of Materials 13 (2001) 2753.
[5] C. Gerardin, N. Sanson, F. Bouyer, F. Fajula, J.L. Putaux, M. Joanicot, T. Chopin, Angewandte Chemie-International Edition 42 (2003) 3681.
[6] L.H. Bronstein, S.N. Sidorov, P.M. Valetsky, J. Hartmann, H. Colfen, M. Antonietti, Langmuir 15 (1999) 6256.
[7] S. Forster, M. Antonietti, Advanced Materials 10 (1998) 195.
[8] H.D. Koh, N.G. Kang, J.S. Lee, Langmuir 23 (2007) 11425.
[9] N. Duxin, F.T. Liu, H. Vali, A. Eisenberg, Journal of the American Chemical Society 127 (2005) 10063.
[10] Y. Guo, M.G. Moffitt, Macromolecules 40 (2007) 5868.
[11] M. Vamvakaki, L. Papoutsakis, V. Katsamanis, T. Afchoudia, P.G. Fragouli, H. Iatrou, N. Hadjichristidis, S.P. Armes, S. Sidorov, D. Zhirov, V. Zhirov, M. Kostylev, L.M. Bronstein, S.H. Anastasiadis, Faraday Discussions 128 (2005) 129.
[12] H. Colfen, Macromolecular Rapid Communications 22 (2001) 219.
[13] J.F. Berret, N. Schonbeck, F. Gazeau, D. El Kharrat, O. Sandre, A. Vacher, M. Airiau, Journal of the American Chemical Society 128 (2006) 1755.
[14] W.J.M. Mulder, R. Koole, R.J. Brandwijk, G. Storm, P.T.K. Chin, G.J. Strijkers, C.D. Donega, K. Nicolay, A.W. Griffioen, Nano Letters 6 (2006) 1.
[15] J.W.M. Bulte, D.L. Kraitchman, NMR in Biomedicine 17 (2004) 484.
[16] M.A. Cohen Stuart, N.A.M. Besseling, R.G. Fokkink, Langmuir 14 (1998) 6846.
[17] A. Harada, K. Kataoka, Macromolecules 28 (1995) 5294.
[18] A.V. Kabanov, T.K. Bronich, V.A. Kabanov, K. Yu, A. Eisenberg, Macromolecules 29 (1996) 6797.
[19] J.F. Gohy, S.K. Varshney, S. Antoun, R. Jerome, Macromolecules 33 (2000) 9298.
[20] L.M. Bronstein, S.N. Sidorov, V. Zhirov, D. Zhirov, Y.A. Kabachii, S.Y. Kochev, P.M. Valetsky, B. Stein, O.I. Kiseleva, S.N. Polyakov, E.V. Shtykova, E.V. Nikulina, D.I. Svergun, A.R. Khokhlov, Journal of Physical Chemistry B 109 (2005) 18786.
[21] F. Bouyer, C. Gerardin, F. Fajula, J.L. Putaux, T. Chopin, Colloids and Surfaces A: Physicochemical and Engineering Aspects 217 (2003) 179.
[22] F. Bouyer, N. Sanson, M. Destarac, C. Gerardin, New Journal of Chemistry 30 (2006) 399.
[23] J.F. Gohy, in: Block Copolymers II, 2005, pp. 65.
[24] I.K. Voets, P.M. Moll, A. Aqil, C. Jerome, C. Detrembleur, P. de Waard, A. De Keizer, M.A. Cohen Stuart, Journal of Physical Chemistry B 112 (2008) 10833.
[25] I.K. Voets, A. de Keizer, P. de Waard, P.M. Frederik, P.H.H. Bomans, H. Schmalz, A. Walther, S.M. King, F.A.M. Leermakers, M.A. Cohen Stuart, Angewandte Chemie-International Edition 45 (2006) 6673.
[26] H. Schmalz, M.G. Lanzendorfer, V. Abetz, A.H.E. Müller, Macromolecular Chemistry and Physics 204 (2003) 1056.
[27] A.J. Convertine, N. Ayres, C.W. Scales, A.B. Lowe, C.L. McCormick, Biomacromolecules 5 (2004) 1177.
[28] P.M. Frederik, D.H.W. Hubert, in: Liposomes, Pt E, 2005, pp. 431.

[29] I.K. Voets, A. De Keizer, M.A. Cohen Stuart, Advances in Colloid and Interface Science 147–148 (2009) 300.
[30] M.A. Cohen Stuart, B. Hofs, I.K. Voets, A. de Keizer, Current Opinion in Colloid and Interface Science 10 (2005) 30.
[31] A. Harada, K. Kataoka, Journal of the American Chemical Society 121 (1999) 9241.
[32] S. van der Burgh, R. Fokkink, A. De Keizer, M.A. Cohen Stuart, Colloids and Surfaces A: Physicochemical and Engineering Aspects 242 (2004) 167.